

Skyeye Team at MBZIRC 2020: A team of aerial and ground robots for GPS-denied autonomous fire extinguishing in an urban building scenario

Simón Martínez-Rozas^{1*}
simon.martinez@uantof.cl

Rafael Rey^{1*}
rreyarc@upo.es

David Alejo^{1*}
daletei@upo.es

Domingo Acedo^{1*}
dacegom@upo.es

José Antonio Cobano¹
jacobsua@upo.es

Alejandro Rodríguez-Ramos²
alejandro.rramos@upm.es

Pascual Campoy²
pascual.campoy@upm.es

Luis Merino¹
lmercab@upo.es

Fernando Caballero¹
fcaballero@us.es

¹**Service Robotics Laboratory**
Universidad Pablo de Olavide
Crta. Utrera, km. 1, 41013, Sevilla, Spain
**Equal contribution*

²**Computer Vision and Aerial Robotics Group**
Centre for Automation and Robotics (C.A.R.)
Universidad Politécnica de Madrid (UPM-CSIC)
Calle Jose Gutierrez Abascal 2, 28006 Madrid, Spain

Abstract

The paper presents a presents a framework for fire extinguishing in an urban scenario by a team of aerial and ground robots. The system was developed for the Challenge 3 of the 2020 Mohamed Bin Zayed International Robotics Challenge (MBZIRC). The challenge required to autonomously detect, locate and extinguish fires in different floors of a building, as well as in the surroundings. The multi-robot system developed consists of a heterogeneous robot team of up to three Unmanned Aerial Vehicles (UAV) and one Unmanned Ground Vehicle (UGV). The paper describes the main hardware and software components for UAV and UGV platforms. It also presents the main algorithmic components of the system: a 3D LIDAR-based mapping and localization module able to work in GPS-denied scenarios; a global planner and a fast local re-planning system for robot navigation; infrared-based perception and robot actuation control for fire extinguishing; and a mission executive and coordination module based on Behavior Trees. The paper finally describes the results obtained during competition, where the system worked fully autonomously and scored in all the trials performed. The system contributed to the third place achieved by the Skyeye team in the Grand Challenge of MBZIRC 2020.

1 Introduction

The application of robotic technologies in disaster management and rescue operations is increasing in the last years due to the advances in the design of platforms and the mapping, localization, perception, planning and coordination capabilities (Delmerico et al., 2019). The goal is to decrease the risks that humans face in such activities and, at the same time, increase the effectiveness of the operations.

Robot competitions are spreading in the world to foster advancements on the research in robotics for these applications and to allow proper benchmarking between different approaches. Some examples related to search and rescue and disaster management scenarios are: the Defense Advanced Research Projects Agency (DARPA) Robotics Challenge (Pratt and Manzo, 2013), RoboCup Rescue competition (Sheh et al., 2016), euRathlon and ERL Emergency (Winfield et al., 2017), DARPA Fast Lightweight Autonomy program (Mohta et al., 2018), Trinity College Robot Competition Schedule Changes (TrinityCollege, 2020) and the Mohamed Bin Zayed International Robotics Challenge (MBZIRC) (MBZIRC, 2020).

Among this kind of missions and challenges, fire fighting is seen as a relevant application of robot systems given the dangerous conditions in which firefighters have to operate. Firefighters are at constant risk of being burned, becoming trapped or inhaling smoke. The risks of losing human lives could be greatly reduced by using autonomous robots capable of searching, detecting and extinguishing the fires. In general, current automatic firefighting systems are fixed. For instance, automatic fire sprinklers and alarms are used in heavily populated and hazardous areas for rapidly extinguishing any fires. Mobile robotic firefighting systems such as ground and aerial robots, on the other hand, could be capable of traveling into areas unsafe and/or inaccessible for people to collect information through on board sensors (visual camera, infrared camera, LIDAR, etc) and even to perform extinguishing operations. This could offer critical new capabilities on real-time situation awareness and remote extinguishing to fire fighters. Achieving this vision still requires, though, advancing the state of the art and robustness of current robots in different directions.

The MBZIRC 2020 competition included a Challenge 3 denoted: “Team of Robots to Fight Fire in High Rise Building”. In it, a team of robots needed to collaborate to detect, localize and extinguish fires in a simulated high-rise building. This involved putting out fires located inside and on the walls of a building at different heights and floors, and outside the building, using water and fire blankets. The mission is challenging and requires to broaden the state-of-the-art in several areas: deployment and coordination of multiple heterogeneous robots (UAVs and UGV) in the same urban workspace; autonomous indoor/outdoor navigation in cluttered environments; autonomous search and location of fires; hardware adaptations and control for fire extinguishing.

This paper describes in detail a multi-robot fully autonomous system conceived for fire extinguishing in such urban high rise building firefighting scenario. The system is composed by two Unmanned Aerial Vehicles (UAV) and one Unmanned Ground Vehicle (UGV). The system ended in 7th position out of 20 teams in Challenge 3 of MBZIRC 2020, and contributed to the 3rd position (out of 17 teams) obtained by the team in the Grand Finale (Grand Challenge), in which this Challenge 3 and the other two Challenges of the competition were run simultaneously and jointly contributed to the final position¹.

The main contributions of the paper are related directly with the components that allowed the system to operate in fully autonomous mode and to coordinate a heterogeneous robot team to address the MBZIRC Challenge 3. First of all, a multi-modal robust localization module, able to operate in GPS-denied scenarios. While the competition allowed the use of GPS and even DGPS (with a penalization in this latter case), the ability to operate without GPS was crucial to be able to navigate autonomously and score in all three trials, given the intermittent reception due to satellite occlusion and other factors. Secondly, a flexible mission composition and execution system based on Behaviour Trees (BT) (Colledanchise and Ogren, 2017). The system is in charge of combining all modules to define the behaviors of each robot and that of the whole team to accomplish missions. This versatility of BTs was fundamental to quickly adapt to the conditions of

¹<https://www.mbzirc.com/winning-teams/2020>

the competition. Finally, the paper also contributes to the robotics community with the description of the specialized navigation, control and perception modules and hardware employed in the competition.

The paper is organised into nine sections. Section 2 describes the hardware designs for the UAV and UGV platforms. Section 3 presents the mapping and localization system implemented. The autonomous navigation system of each platform is described in Section 4. Section 5 shows the approach proposed to detect and extinguish the fires and Section 6 presents the framework used to carry out the mission. Experiments are presented in Section 7. Finally, lessons learned and conclusions are described in Section 8.

1.1 State of the art

The idea of using robots for fire fighting has been present in the community for many years. Early designs can be traced back to (Bradshaw, 1991), which describes the functional and mechanical design of a ground robot for fire detection and first intervention in indoor environments. In (Amano et al., 2001), the authors show the design of a climbing robot for helping fire activities in buildings. All in all, robots are considered as a promising tool to fight fires because of their ability to reach inaccessible zones, assist in dangerous environments in addition to carry sensors to monitor and control the fires.

Actually, robotic technology is being often deployed as part of firefighting operations in the last years. Current examples can be found in the Notre Dame fire in 2019 with the firefighting ground robot called Colossus². It is a remote-controlled firefighting automaton designed and built by Shark Robotics. TC800-FF is another remotely operated ground robot with some autonomous navigation capabilities designed to assist fire-fighter during operations³. Two of the most popular firefighting ground robots are the Thermite RS1-T3 and RS2-T2⁴. The aim of all these robots is to replace fighters and to keep them safe and free from the heavy work that distracts them and takes time away from solving problems quickly and effectively. Most of these systems are mainly teleoperated. While teleoperation can be enough for certain scenarios, the inclusion of autonomous capabilities expand further the utility of such systems.

Furthermore, in the case of high-rise buildings and in other scenarios, the use of aerial robots can be beneficial. In the last 15 years, Unmanned Aerial Vehicles (UAVs) have been more and more used in wildfire fighting (e.g. (Ambrosia et al., 2003; Casbeer et al., 2006; Merino et al., 2006; Skeeel and Hollinger, 2016; Bailon-Ruiz et al., 2018)). These systems are mainly used as “eyes in the skies”, to provide situational awareness to first response teams, given their capability of carrying sensors and position in vantage points. Some of these works (Casbeer et al., 2006; Merino et al., 2006; Bailon-Ruiz et al., 2018) have shown the advantages of using teams of cooperating UAVs for fire fighting. In particular, we have also shown in our former works (Merino et al., 2006; Merino et al., 2012) the added value of cooperating heterogeneous UAVs with different capabilities and that can carry complementary sensors in order to localize precisely fire spots and discard false alarms. Currently, drones are used as part of wildfire operations, as for instance during the Australian bushfires where drones were used to search and rescue koalas affected by the fires.

Those works do not consider the inclusion of fire suppression mechanisms, which for UAVs is also a challenge. A novel hose type robot, which can fly directly into the fire source via a water-jet, has been proposed in (Ando et al., 2018). In (Yamada and Nakamura, 2016) the concept of attaching a drone to the tip of a fire hose and remotely extinguishing a fire is presented. These studies have not been tested in a real fire extinguishing task. Problems such as the payload and influence of the tension of the hose itself on the flight must be addressed to bring the UAV’s hose closer to the fire source.

When considering the use of autonomous robots to fight urban fires in buildings, additional challenges are present, like the navigation in GPS denied or with limited GPS cluttered scenarios, as is typically the case in urban canyons and/or close to and inside buildings, and the operation in low-visibility conditions (Schneider

²<https://www.shark-robotics.com/colossus>

³<https://www.robotpompier.com/en/>

⁴<http://www.roboticfirefighters.com/>



Figure 1: Arena of Challenge 3. There are simulated fires on the facades of the building (top-left), and inside the building (down, right), located on the ground, first and second floor (to be suppressed with water). There are also fires located on the ground outside (down, left) that need to be suppressed with a blanket.

and Wildermuth, 2017). The last years have seen important advances in the navigation of UAVs in GPS-denied scenarios (for instance (Shen et al., 2014; Mohta et al., 2018; Perez-Grau et al., 2018; Usenko et al., 2020)), allowing their use in this kind of scenarios.

The cooperation between UAVs and UGVs offers additional challenges. In (Michael et al., 2014) the synergies between a UGV and UAVs are exploited to map buildings affected by earthquakes. However, in the literature there are not many works for fire fighting in urban environments with fully-autonomous ground and aerial robots. In (Maza et al., 2011), a system of multiple UAVs cooperating with a static sensor network for a fire scenario in a building is presented. UAVs are used to deploy new sensors and provide situation awareness, which is then used to attack the fire by firefighters. The work shows again how cooperation can be very valuable. The system assumes GPS coverage, no ground robots are considered, and no extinguishing is performed by the robots themselves.

In summary, there are many researches on the UAV and UGV application in fire detection and rescue operations, but no many researches have tackled the fire emergencies by applying teams of UGV and UAV in firefighting in urban environments.

1.2 Problem statement

This section summarizes the main aspects of the rules, conditions and scoring of the MBZIRC Challenge 3, which requires a team of UAVs and UGV collaborating in order to autonomously extinguish a series of simulated fires in an urban high rise building firefighting scenario⁵. Figure 1 shows the arena for Challenge 3, with a size of approximately that of half a football pitch. A 15-meter high structure simulates the building.

The robots have to extinguish a set of 6 fires located in the 3 floors of the building using water. For each floor, there is one fire inside the building and one fire on the facade (see Fig. 1). Furthermore, there are 2 fires located at ground level outside the building that must be extinguished using fire blankets carried by the robots. The locations of the fires are changed randomly between trials. Each fire is scored between 0 and 1. For the fires in the building the maximum score is obtained if the amount of water properly thrown into the fire is 1 liter. Simulated fire spots on the ground score when they are covered with a blanket (with a maximum when they are totally covered). The final score is obtained by a weighted sum for all 8 fires.

⁵<https://www.mbzirc.com/challenge/2020>

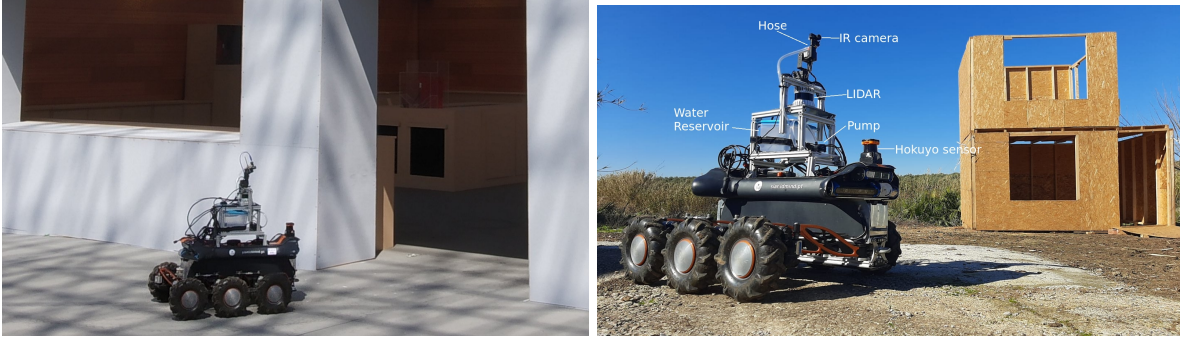


Figure 2: Ground platform used for Challenge 3.

Different fires receive different weights according to their difficulty⁶.

The mission can be attempted in either fully autonomous or manual mode. The mission is considered in manual mode from the moment there is an intervention by a human on (the only interventions allowed are to replenish water and change batteries and blankets). Any score in manual mode is considered below a score in autonomous mode, or to disambiguate in case of draw for scores in autonomous mode. GPS is allowed. RTK/DGPS can be used although a penalty of 25% will be applied if it is used.

The duration of Challenge 3 is 15 minutes and of the Grand Challenge 25 minutes, with a 5-minute preparation slot. The Grand Challenge is a triathlon type event in which a fleet of up to 3 UAVs and 1 UGV addresses the three challenges at the same time.

2 Hardware

The robot team to address the challenge consists of one UGV and up to 3 UAVs. They are adequately equipped to perform navigation and to detect and extinguish the fire for this firefighting scenario.

2.1 Unmanned ground vehicle

The ground platform used is called SIAR (Alejo et al., 2020), a 6-wheeled robot with independent traction system and a pan&tilt mechanism on top. The robot is able to navigate at a maximum speed of 0.7 m/s and it has battery autonomy for more than 4 hours of operation (motion and sensing/computation). The robot integrates an i7 computer, local sensing and a 3D LIDAR. The main sensors and mechanisms used in the ground platform are (see Fig. 2):

- GPS sensor UBlox 8 and ArduIMUv3 Inertial Measurement Unit (IMU).
- LIDARs: A 3D OS-1-16 LIDAR manufactured by Ouster has been installed on top of the robot. The LIDAR is able to provide 320k 3D points per second, ranging from 0.2 to 120 meters. The information gathered by this sensor is used for localization and mapping. Furthermore, a Hokuyo UTM-30LX 2D sensor is installed. The information of this sensor is used for local obstacle detection/avoidance.
- Cameras: A SeekThermal IR camera to detect the sources of heat and an Orbbec's ASTRA camera that provides the operator with images to operate the platform if needed.
- Pan&Tilt unit: It moves the thermal camera for searching and centering the fire, and at the same time, it holds and guides the hose of the extinguishing system to aim the fire.

⁶<https://www.mbzirc.com/scoring-scheme>

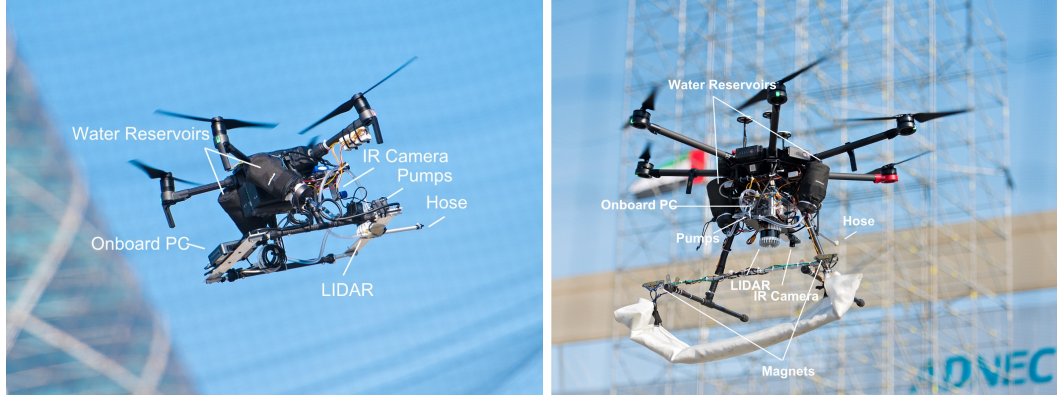


Figure 3: Left: Adapted DJI Matrice 210v2 for facade fire extinguishing, with LIDAR and PC placed to avoid blocking the down-looking sensors. Right: Adapted DJI Matrice 600 for blanket deployment and facade fire extinguishing.

- **Extinguishing System:** It consists in a series connection of two water pumps (5V, 4.8 W ,300cm Hmax,300L/H, no valve), one MOSFET module 5V, hoses, and a 3-liter water tank (within the limits of the competition). To improve the intake of water, the tank is placed above the water pumps. Alike, the output hose is placed above the pump to prevent the water from going out, as the pumps do not have a valve. With this, we have a system that ejects water 2 meters in a straight line from the hose outlet

2.2 Unmanned aerial vehicles

Regarding to the aerial platforms, the aerial robot models used for the competition are adaptations of the DJI Matrice 210 V2 and the DJI Matrice 600 Pro (see Fig. 3). We selected these platforms because of the robustness of the hardware and software, support that the provider offers, and also their facility to communicate the PC on-board with the Robot Operating System (ROS) (Quigley et al., 2009). The drone's structure was adapted in order to perform the tasks and allow to integrate new hardware. For that, we take into account the maximum weight that can carry each drone and also the dimension constraints of the competition.

Each UAV robot integrates an i7 NUC computer and local sensing. The main sensors and mechanisms added to the UAVs are (see Fig. 3):

- **DJI Matrice onboard sensors.** This includes single GPS, Inertial Measurement Unit (IMU) and barometric altimeter. DJI Matrice 600 intergrates 3 GPS receivers and 3 IMUs for redundancy and fault detection purposes, but they behaves as single devices.
- **3D LIDAR.** OS-1-16 LIDAR by Ouster. The purpose of this sensor is threefold: environment mapping, localization and odometry. It is the basis for the generation of the 3D map of the environment, and to compute an accurate robot odometry in the UAVs. It is also used as main sensor for robot localization in all robots and to detect obstacles by the navigation module.
- **Infrared camera:** SeekThermal whose images are used for fire detection. The M210 carries one looking forward, while the M600 carries another one in a nadir configuration for the ground fires.
- **Water Extinguishing System:** we use the same pumps as the UGV platform, but with less capacity due to payload constraints. We use two 0.5-liter water tank, which are positioned on each leg of the drone to evenly distribute their weight. The outlet of the tanks are joined in a coupling that

carries the water to the pumps. These are located in a structure below the drone and the tanks. An aluminum tube is used to guide the outlet hose from the pumps to a safe area in which the air turbulence generated by the drone itself does not disperse the water when it is ejected. A flow restrictor is placed at the outlet of the hose to increase the pressure and range.

- Blanket Extinguishing system (M600 only): we use six electromagnets to carry and drop the blanket. The electromagnets are located on a bar that joins the back of the two legs of the drone. The blanket is transported rolled up to prevent the air turbulence generated by the drone from producing a sail effect. The electromagnets are distributed into two groups of three electromagnets each. In each group there is one for rolling the blanket and two for dropping it. When desired, the rolling electromagnets are deactivated and the blanket is unrolled, and when the blanket is to be thrown, the drop electromagnets are deactivated.

3 3D Mapping and Localization

One of the main issues in Challenge 3 is the localization of the robots. They should localize seamlessly and accurately in GPS and GPS-denied environment (inside the building, urban canyons and, in general, areas with high dilution of precision), with a smooth transition among them.

The mapping and localization system proposed consists of two main components: a LIDAR-based odometry and an online map-based global localization module. These systems create the global map during the mapping phase, and estimate the global position of the robot into the map during the mission. While there are differences in the implementations for the UAVs and UGV, the modules are based on the same principles.

3.1 3D Mapping and multi-sensor odometry

The base for the mapping and localization systems is an odometry system that allows to estimate the relative motion of the robot. The LIDAR-based odometry module considers IMU and 3D LIDAR in order to compute a reliable 6DoF robot odometry in the environment. This module provides short-term aligned scans that can be used for local mapping, and a map of the environment. It integrates the IMU estimation together with a LIDAR-based mapping process to provide global consistency to the mapping process.

The LIDAR-based odometry module implements a LIDAR Odometry and Mapping (LOAM) system (Zhang and Singh, 2014), which decomposes the original SLAM problem into scan registration and mapping. The first problem is solved as online motion estimation. The second one conducts mapping as batch optimization (similar to iterative closest point, ICP (Rusinkiewicz and Levoy, 2001)). The system computes high-precision motion estimates and maps. We make use of an open software implementation of the original LOAM system (Zhang and Singh, 2014)(Zhang and Singh, 2017), it can be found here⁷. This implementation integrates Ceres Solver for non-linear optimization (Agarwal et al., 2012), it also improves the integration with ROS.

A drone equipped with LIDAR, GPS and on-board sensors (IMU, altimeter, etc) was flown manually over the Challenge 3 arena during the first rehearsal, mapping the environment at different altitudes, from the 2 meters approximately to the building top. The resulting 3D map is shown in Fig. 4. During the mapping stage, the information from the GPS is used to compute the relative transformation between the map-based global frame and the GPS coordinate system for multi-sensor localization.

3.2 Multi-sensor robot localization

The localization module provides a robust global position of the robot within the built map. The algorithm is based on a Monte Carlo localization (MCL) (Thrun et al., 2001) approach that extends our previous work

⁷<https://github.com/HKUST-Aerial-Robotics/A-LOAM>

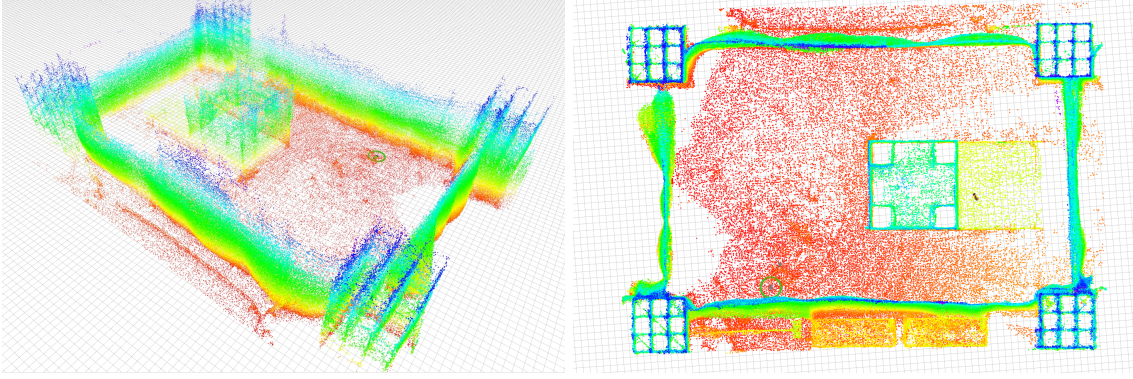


Figure 4: Two views of the map generated for the Challenge 3 of the scenario shown in Fig. 1 with data provided by the M600 UAV. It can be seen how the system is able to accurately map the interior of the building and also the four scaffolding structures in the corners.

presented in (Perez-Grau et al., 2017) with new sensors updates and with a different approach multiple sensor weighting integration. The source code of the version used in the experiments is publicly available⁸.

The localization filter maintains N pose hypotheses (particles) p_i , each one with the following state vector $p_i = [x, y, z, \Psi]_t$, where Ψ refers to the yaw angle of the robot. Each particle has an associated weight w_i such as $\sum_i^N(w_i) = 1$. Note how the robot roll and pitch angles are not included into the robot pose definition. These angles are available and accurate enough in the robot through the use of its onboard IMU. They are fully observable and their values are usually accurate. This greatly reduces the computational complexity of the algorithm, allowing for real-time onboard computation.

The particles are initialized by setting the initial pose (at the take-off spot) and distributing them in the hypotheses space. The LIDAR-based odometry provides increments of the robot pose on the robot frame (after roll and pitch compensation) $[\Delta x, \Delta y, \Delta z, \Delta \Psi]$, which are used to propagate the distribution of the particles at each time step. Thus, the state of the particles will evolve according to the following expressions for particle i :

$$x_i^{t+1} = x_i^t + \Delta x \times \cos(\Psi_i^t) - \Delta y \times \sin(\Psi_i^t) \quad (1)$$

$$y_i^{t+1} = y_i^t + \Delta x \times \sin(\Psi_i^t) - \Delta y \times \cos(\Psi_i^t) \quad (2)$$

$$z_i^{t+1} = z_i^t + \Delta z \quad (3)$$

$$\Psi_i^{t+1} = \Psi_i^t + \Delta \Psi \quad (4)$$

The values of Δx , Δy , Δz , and $\Delta \Psi$ are drawn randomly following a normal distribution centered in their actual values and standard deviations proportional to each increment itself.

The approach evaluates the sensors only when the robot moves above given thresholds in both translation and rotation. When the robot moves above one or both thresholds, it performs an update: using the previous equations to predict robot position according to odometry, updating particles based on sensors and re-sampling the hypotheses space when required. The following sensor readings are used to update the weight associated to each particle's hypothesis: the point clouds provided by the 3D LIDAR sensor, the 3D position provided by the GPS, the robot roll, pitch and yaw provided by the IMU and the height above the ground provided by the altitude sensor. Each sensor is integrated into the MCL as follows:

⁸<https://github.com/robotics-upo/mcl3d>

- The point clouds are transformed to each particle pose in order to find correspondences between the cloud and what the map should look like from that particle's pose. Since this is very expensive computationally, we first compute a 3D probability grid as in (Hornung et al., 2010; Perez-Grau et al., 2017), in which each position stores a value of how likely it is that such position falls within an occupied point of the map, instead of storing binary information about occupancy as in the provided map. Each 3D position \mathbf{p}_i of the grid is then filled with probability values according to a specific Gaussian distribution centered in the closest occupied point in the map from \mathbf{p}_i , \mathbf{map}_i , and whose variance σ^2 depends on the sensor noise used in the approach.

$$grid(\mathbf{p}_i) = \frac{1}{\sqrt{2\pi\sigma^2}} e^{-\|\mathbf{p}_i - \mathbf{map}_i\|^2 / 2\sigma^2} \quad (5)$$

Such probability grid only needs to be computed once, it is not required to be updated for a given environment, and relieves from performing numerous distance computations between each cloud point for each particle and its closest occupied point in the map. Besides, each point cloud is first transformed according to the current roll and pitch provided by the on-board IMU. This transformation is done just once per update, reducing the computational requirements as well. Then, for every point of the transformed cloud, we access its corresponding value in the 3D probability grid. Such value would be an indicator of how likely is that point to be part of the map. By doing this with every point of the cloud and adding all the probability values, we obtain a figure of how well that particle fits the true location of the aerial robot according to the map.

Finally, the weight w_i of each particle \mathbf{p}_i is computed. Assuming that the point cloud is composed of M 3D points \mathbf{c}_j , the weight is computed by adding the associated probability grid values:

$$w_i^{map} = \frac{1}{M} \sum_{j=1}^M grid(\mathbf{p}_i(\mathbf{c}_j)) \quad (6)$$

where $\mathbf{p}_i(\mathbf{c}_j)$ stands for the transformation of the point to the particle's state, and $grid(\mathbf{p}_i(\mathbf{c}_j))$ is the evaluation of the probability grid in such transformed position.

Equation (6) can be also computed as the product of all $grid(\mathbf{p}_i(\mathbf{c}_j))$, however this was discarded for the following reasons: a) outlier points \mathbf{c}_j might have a significant impact in the weight computation, leading to almost zero in some cases, b) point clouds area easily composed by dozens of thousands of points, given that $grid(\mathbf{p}_i(\mathbf{c}_j))$ ranges from 1 to 0, we can fall into numerical errors in the product.

- The position measurements provided by the GPS are used to check how well each particle matches the sensor reading. First, the GPS position is transformed into the map by means of a known fixed transformation computed during mapping task. Then, a w^{gps} is computed for each particle. Assuming a GPS measurement \mathbf{p}^{gps} , the associated weight w_i^{gps} is computed as follows:

$$w_i^{gps} = \frac{1}{\sqrt{2\pi\sigma^2}} e^{-\|\mathbf{p}_i - \mathbf{p}^{gps}\|^2 / 2\sigma^2} \quad (7)$$

where the distance computation dismisses the altitude contribution of the GPS, which is subject to significant noise. Also, the standard deviation of the GPS measurement σ is computed empirically from the data gathered during the mapping stage and to account for GPS errors in single configuration.

- The height above the ground is integrated into the MCL through the re-sampling stage. Instead of including the information as a regular update, we decided to include this information into the re-sampling, forcing the hypotheses to be distributed around the altitude provided by the robot altimeter. This way, we can reduce the dispersion of the particles around Z axis, which is easily observable by means of sensors such as laser altimeter, barometer or GPS.
- IMU yaw angle is also integrated through the re-sampling stage. The rationale behind this decision is also based on the computational optimization and the nature of the yaw angle. In the experiments

area, the yaw angle was checked to be only slightly distorted by the environment, so that we can trust the estimation from the magnetometer. Thus, every time a new re-sampling is performed, the orientation of the particles are drawn from a Gaussian distribution centered in the latest yaw value provided by the IMU. A global to map calibration is used to transform the IMU yaw into the map yaw.

As mentioned, GPS and point-cloud updates are integrated into the filter. Given the distinct nature of the two technologies involved, we calculate separate weights for each sensing modality. A weighted average is used to obtain the final weight of each particle:

$$w_i = \alpha * w_i^{map} + (1 - \alpha) * w_i^{gps} \quad (8)$$

where α is chosen depending on the particularities of the indoor environment where the robot is going to operate. If the map used in the MCL does not contain the full environment or its accuracy is not enough to trust the map matching, α should be lower than 0.5. Whereas if GPS measurements are not accurate, α should be higher.

As a result of the rehearsal experiments in the MBZIRC arena, the value of the w^{gps} was initially set to a value lower than 0.5 to account for the inaccuracies and BIAS induced in the GPS estimation in this particular place. Actually, the value of w^{gps} was finally set to 0 during the trials due to its error BIAS, leading to a complete GPS-free localization approach.

This approach is used for both robot systems, ground and aerial. However, the dispersion in Z axis is set to a very small value in the predictive model of the ground robot. This relates with the fact that the UGV moves in 2D.

4 Autonomous robot navigation

One key capability is to position the robots of the fleet on arbitrary free poses on the map autonomously. The implemented autonomous navigation system is divided into a global and a local planner. Planning is done in 3D for the UAVs and 2D for the UGV. The Global Planner computes a global path on the map frame. The inputs are the goal to be reached, the static global map of the environment and the current robot localization given by the MCL approach. For the UGV, we use a 2D traversability map derived from an analysis of the 3D map. The output is a feasible and safe path that should be followed in order to reach the goal.

The Local Planner is in charge of following the global path and dealing with dynamic and unmapped obstacles detected by the onboard 3D LIDAR. It takes as input the global path and a local map built by using the measurements of the onboard sensors. The size of the local map considered in the 2D case is 6x6 meters and in the 3D one is 6x6x2 meters. As output, it provides a free-collision local trajectory to the path tracker module. We need fast planning capabilities, as in the case of the local planner a new local plan should be generated whenever a new LIDAR measure is obtained (and therefore a new local map is generated), at an approximate rate of 10Hz. Thus, both planners are based on the Lazy Theta* algorithm (Nash and Tovey, 2010), a fast and reliable heuristic planner. An advantage of the Lazy Theta* algorithm is the optimization of its computational load, and its high repeatability. These characteristics make this algorithm suitable to address the tasks of the MBZIRC competition.

First, the planner manages the inflation of the nodes in each dimension to generate the trajectory and check if the initial or final node are occupied. In that case, it should explore alternative nodes to compute the trajectory. Then, the path planning algorithm is launched and a collision-free trajectory computed.

The original Lazy Theta* algorithm has been modified. Our algorithm fosters safety instead of the classical optimal-length path. In particular, we modified the Lazy Theta* algorithm in the following ways:

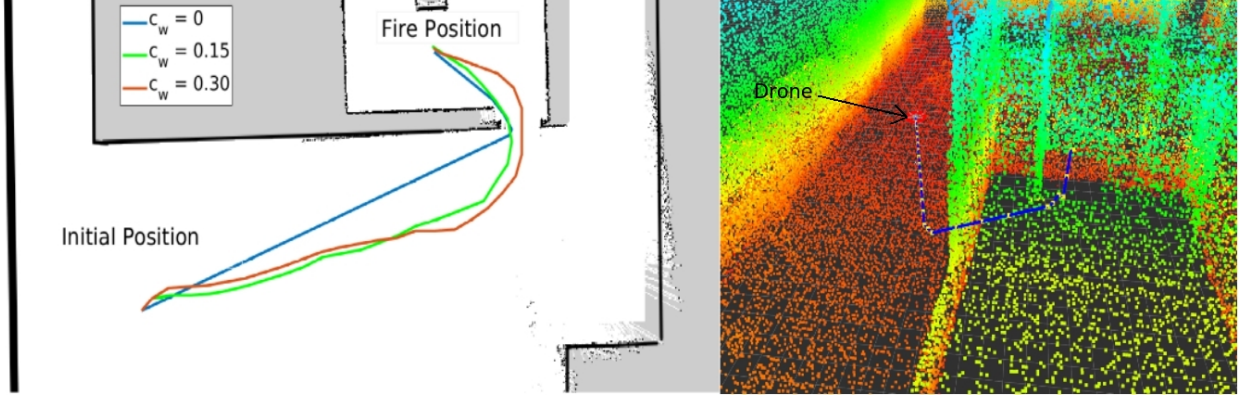


Figure 5: Left: 2D Global paths computed for the UGV coming into the building (2D map of navigation) by considering different values of the cost factor, C_w . Right: 3D Global path computed for the UAV coming into the building in the first floor.

- **Cost to reach a node.** We added a cost component to the Euclidean distance in the original algorithm. For each node in the grid, this cost is distance to the nearest obstacle. Then, the cost to reach a node is now a sum of the Euclidean distances and the new cost component for the nodes that define the trajectory. The latter component is weighted by a weight factor C_w between 0 and 1. This results in paths with larger safe margins with respect to obstacles, depending on the value of the weight factor.
- **Line of sight.** The line of sight is limited in order to allow the algorithm to link two nodes only if they are not further than a given distance. Otherwise, the first modification would have no effect because the original algorithm checks if there is a direct line of sight between nodes regardless of the cost. Therefore, the algorithm would undo the changes in the cost if the line of sight is not limited.

These two modifications provide paths with larger safety margins with respect to obstacles at the cost of exploring more nodes. The quality and the computation time of these paths depends on the weight factor and maximum line of sight distance, so the values of these parameters have been chosen in order to maintain a low computation time and generate safer paths. Figure 5-left shows trajectories computed with different weight factors and a maximum line of sight distance of 1.5m. Concretely, the factor, C_w , finally chosen is 0.15 because it generates a safer trajectory than the one obtained with the original algorithm (blue line). This can be appreciated when robot crosses the door. The advantage of the trajectory computed with $C_w = 0.15$ with respect to $C_w = 0.3$ is that the first one requires less computation time because less nodes are explored. In addition, it is also a good compromise solution between safety and trajectory length. Fig. 5-right shows a screenshot of a 3D global path generated for UAV coming in the building in the first floor through a window. The weight factor was finally set to 0 during the competition in the case of the UAVs to achieve the required frequency for the local 3D planner.

Finally, the Path Tracker module computes the velocity commands to navigate and follow the trajectory computed by the Local Planner in both platforms. The UGV makes use of a pure pursuit controller that adapts the angular and linear velocity of the robot to reach the closest point into the commanded trajectory. On the other hand, the UAVs make use of the command velocity interface provided by the DJI software. This interface allows commanding linear velocities in X, Y and Z axes, and angular rates in yaw. A simple controller has been implemented to follow the commanded local trajectory in the UAVs, in which a trapezoidal velocity profile is applied over each axis in order to reach the closest point of the commanded trajectory.

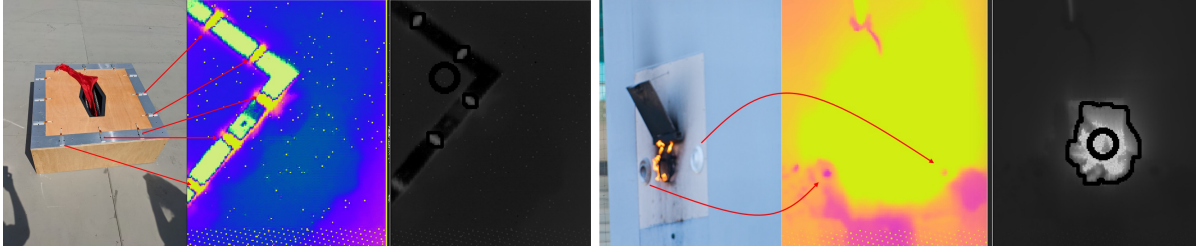


Figure 6: Left: simulated ground fire, colored temperature image and segmentation using the radiometric values (the circle shows the mean position of the fire). The fire is simulated by a set of heaters connected to a metallic plate. However, the emissivity of such metal makes it look cooler than the surroundings. Right: simulated facade fire, colored temperature image and segmentation using the radiometric values. The original temperature image gets saturated, while working with the radiometric field allows for a detailed segmentation.

5 Fire perception and extinguishing

Our approach the extinguishing fire task in the MBZIRC - Challenge 3 consists of two modules: the perception module detects fires and estimates their positions with a thermal camera; and an extinguishing module that attacks the fire by dropping a blanket or ejecting water.

5.1 Fire perception

The module of fire perception detects fires within the scene using as input the data from a thermal camera. As output, it indicates if a fire has been detected, as well as its 2D coordinates on the image plane and 3D coordinates in the scenario.

All fires in the competition were simulated using a thermal heated plate that reached temperatures up to 110° . The fires on the facades featured additionally a real fire using gas, while the remaining fires were also visually simulated by using a flame simulator using a red silk.

In our solution, we aimed for a fully infrared-based detection of the heat source. The main sensor related to fire perception is the miniature infrared thermal camera from Seek Thermal mentioned above. The camera can detect temperatures between -40° to 330° Celsius. We forked a ROS driver from ETHZ and made additional modifications⁹. The driver provides a grayscale temperature image, as well as a radiometric map.

Fire detection is carried out by analyzing the images provided by the infrared cameras. A calibration procedure transforms the raw radiometric data obtained by the cameras to temperature ranges. While obtaining absolute temperature values from radiometry is a very complex process, dependant on the material emissivity (for instance, a metal can radiate less IR energy for the same temperature than other materials with larger emissivity), atmospheric attenuation, and many other factors, here we are more interested on clear relative temperature differences, which simplifies the calibration procedure. The calibration is performed for the different kind of fires once. Then, given the clear difference of temperatures between the fire and the surroundings, a thresholding operation is performed to segment the fire pixels. As a result, the fire detection module provides coordinates on the image plane of fire spots. Fig. 6 shows detection results obtained during the competition.

⁹https://github.com/robotics-upo/seekthermal_ros

5.2 Fire position estimation

The fire segmentation results mentioned above will be used for the visual servoing final approach to extinguish the fire (see Section 5.3). However, during the exploration of the scenario we need to estimate the 3D position of the fire spots to plan the approximation goals for fire extinguishing.

From the fire position in pixel coordinates it is not possible to estimate the 3D position of the fires, as there is no information about the range to the fires. In order to obtain the range, the LIDAR information is considered. The LIDAR values are mapped to the image coordinates given the known static transformation between sensors and camera internal calibration. This way they can be associated to the fire object, so that a range can be estimated. This is not always possible given the resolution of the LIDAR (and depending on the actual distance to the fire). If not range information is available, the range is estimated considering the maximum distances according to the 3D map of the environment. For the fires located on the floor, the height of the UAV is considered to estimate the position of the fire.

Each measurement is associated with a covariance matrix that reflects the uncertainty on the range, which is adapted according to the estimated range (when no range is available, a large uncertainty is associated to the range), and other aspects like the position of the robot. Then, an Information Filter is used to fuse in time the measurements about the position of the fire from different view points in order to triangulate the fire position, as in our previous work (Dias et al., 2015).

5.3 Fire extinguishing

This module is in charge of confirming the fire presence, aiming adequately the extinguisher system, and releasing the water or the blanket. The module assumes that the robot is already located at an attacking distance to the fire. Three tasks should be accomplished separately in each robot: confirming, centering and extinguishing.

5.3.1 UGV - Water ejection

The water ejecting strategy begins by performing a scan with the Pan&Tilt unit onboard the UGV to look for the precise position of the fire. To this end, we command a predefined trajectory to the pan and tilt unit using position commands. At this point, the Fire Detection module is activated.

Whenever the Fire Detection module reports a fire, we use a velocity visual servoing proportional control for the Pan&Tilt unit so that the detected position on the image plane of the fire enters into the locked on target zone. We have empirically defined this zone in such a way that the water ejecting mechanism hits on target. This zone is indicated in an area of the image and it depends on both the height and distance to the target.

Once the extinguisher has locked on the fire, we start to eject water. As a final note, it is difficult to perceive the trajectory of the water with the onboard sensors. Thus, to increase the chances of successfully hitting the target, the pan&tilt unit performs a cross-shaped movement while ejecting water during 60 seconds.

5.3.2 UAV - Water ejection

To extinguish the fires on the facade, once the UAV is positioned in the attack position, the UAV first performs a manoeuvre to confirm that there is a fire in the area (to compensate for imprecision on reaching the fire attacking waypoint or on the estimated 3D fire position). This manoeuvre consists of performing a square motion parallel to the facade of the building.

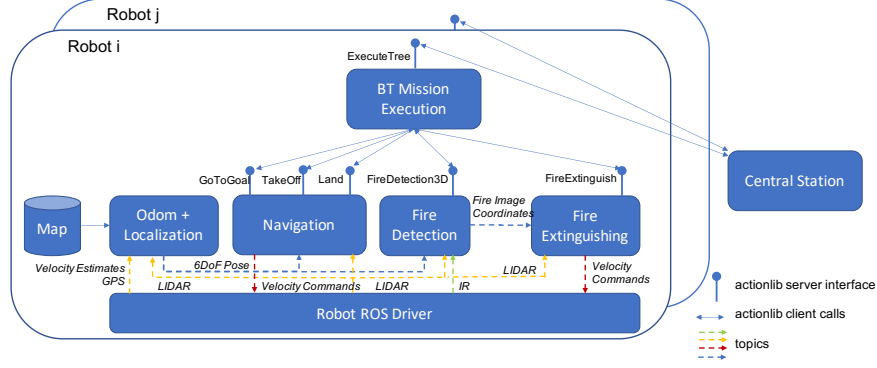


Figure 7: A depiction of the architecture. Each robot has operation autonomy to execute missions, and all processing takes place onboard, where all modules enclosed in the figure run. A central Control Station can order the robots to execute missions through the Mission Execution node.

As soon as a fire is detected the square sequence stops. We use a proportional velocity controller in the local Y and Z axes so that the detected position of the fire on the image plane enters into the locked on target zone. As in UGV, we have empirically defined the locked on target area on the image assuming a distance of attack to the fire. Once the fire is on the locked on target zone, the water ejecting starts. As the UAV can be subjected to disturbances while flying which may cause the UAV move outside the lockup zone, the velocity controller keeps regulating the position during the ejection.

For the fires inside the building, as before, first the drone starts a fire confirmation sequence. In this case, to prioritize the safety of the platform, the maneuver consists just of yaw rotations in place. If a heat trace is found, then a proportional velocity controller in yaw is executed to center the fire horizontally on the image plane. When this is achieved the water ejecting starts, keeping the controller for correcting disturbances.

5.3.3 UAV - Blanket disposal

Again, the UAV performs a confirming fire manoeuvre similar to the one done for facade wall fires, but this time the UAV moves in a plane parallel to the ground. As the blanket must cover the fire, the extinguishing action is more tricky. Once the fire is confirmed on the image, the UAV is placed just above the fire. Then the drone descends to be more accurate when dropping the blanket. Afterwards, the UAV moves backwards until the fire is out of image and stop. Just in that moment, two electromagnets from the extinguishing system switch off to unroll the blanket. From there, the UAV moves forward passing throw the fire, and so detecting the fire again with the thermal camera. The UAV will continue this movement, over passing the fire, and just when the thermal camera stop detecting the fire, the last four magnets will switch off and so the blanket drops covering the fire. From there, a fast move upward is performed in order to avoid any collision with the deployed blankets.

6 Mission Executive and Multi-Robot Coordination

6.1 Integration

All former components need to be integrated and work jointly to achieve the missions of the Challenge. This integration relies on the ROS framework, using the `ros-kinetic` distribution under Ubuntu 16.04. The algorithms described above have been implemented as ROS nodes.

The basic architecture of the system is shown in Fig. 7. Continuous data flows between nodes are im-

actionlib	Params	Final Status	Result
TakeOff	Height	CANCELLED if vehicle not ready SUCCEEDED if height reached ABORTED if height cannot be reached after takeoff	None
Land	None	CANCELLED if vehicle already landed SUCCEEDED landed ABORTED if the UAV cannot land	None
GoToGoal (Section 4)	Waypoint (WP)	CANCELLED if no path to WP SUCCEEDED if WP reached ABORTED if WP cannot be reached	None
FireDetect (Section 5.1)	Duration	SUCCEEDED if fire found within the given duration ABORTED if fire not found	3D position of fire
FireExtinguish (Section 5.3)	None	SUCCEEDED if fire can be locked on ABORTED if fire cannot be locked on	None

Table 1: Atomic tasks that can be carried out by each robot. Actionlib interface, parameters required, potential final status, and final result reported.

plemented through ROS topics. Some of these nodes also provide atomic tasks that will be composed to create the whole missions. To provide the interface to such tasks, we employ the ROS’ `actionlib` package¹⁰, which offers a simple interface to preemptable tasks. In particular, we use the task model offered by the `SimpleActionServer` implementation (actions can be **ACTIVE** when running; **SUCCEEDED** when successfully finished; **CANCELED** if they cannot be processed; **ABORTED** if they cannot be completed; finally, actions can be also **PREEMPTED** by the client). The list of atomic tasks considered by each robot are shown in Table 6.2. These tasks are the same for all robots, but of course they have specialized implementations depending on the robot (for instance, **TakeOff** is not applicable to the UGV, and the **FireExtinguish** action has the three variants described in Section 5.3).

6.2 Mission definition and execution

Given the atomic tasks that can be carried out by the modules described above, we need a framework to combine, execute and supervise them to carry out the mission. We employ Behaviour Trees (BTs) as the framework for mission definition and execution for the robots of the team.

BTs are a way to structure the flow and control of multiple tasks in the context of decision-making applications. They are usually presented as an alternative to Finite State Machines (FSM) that offer advantages in terms of modularity and reactivity. First originated as a tool for Non-Player Character (NPC) AI development in the video game industry, BTs have become widespread in robotics, mainly due to its modularity and simplicity (Colledanchise and Ogren, 2017; Paxton et al., 2017; Colledanchise, 2018), including their use to define behaviours for UAVs (Ogren, 2012; Molina et al., 2020).

While a full description of the BT framework is out of the scope of this paper, here we summarize its main elements. BT model behaviors as hierarchical trees made up of nodes (an example can be seen in Fig. 8). Trees are traversed from top to bottom at a given tick rate following a set of well-defined rules and executing the tasks/commands associated to the nodes that are encountered while doing so. Nodes’ statuses are reported back up in the chain and the flow changes accordingly. A status can be either **SUCCESS**, **FAILURE** or **RUNNING**. According to their functionality, nodes can be classified as:

- **Composite**: it controls the flow through the tree itself and are similar to control structures in structured programming languages.

¹⁰<http://wiki.ros.org/actionlib>

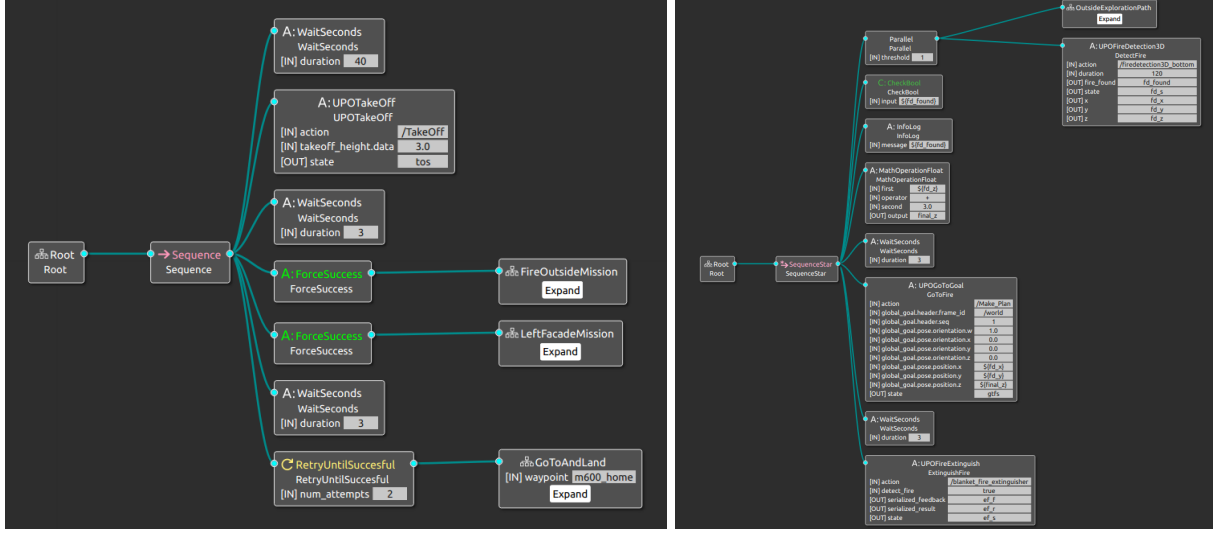


Figure 8: A (simplified) BT for the M600 mission. The robot is tasked with putting out one outside fire and then a fire on one of the facades of the building. Left: general tree. The **Sequence** composite node executes the leaves from top to bottom. If some node returns **FAILURE**, the whole mission fails. The UAV takes off after a timeout (to wait for the ground robot to be at a safe distance). Then, the fire outside submission is carried out. The **ForceSuccess** decorator forces to return **SUCCESS** regardless of the result, as we want the UAV to carry out with the rest of the mission. Then, the robot is tasked to the facade fire extinguishing mission. Regardless of the result (through the second **ForceSuccess**), the robot will go back to the home position. Please notice the leaf nodes **FireOutsideMission**, **LeftFacadeMission** and **GotoAndLand** are themselves sub-behaviors, which illustrate the composability. Right: **FireOutsideMission** subtree. First, the **Parallel** composite node executes (ticks) in parallel a path to explore (**OutsideExplorationPath**, which uses the navigation actions of Section 4) and activates the **UPOFireDetection3D** action of Section 5. Once one of the two nodes returns **SUCCESS**, the **Parallel** composite returns **SUCCESS** (**FAILURE** otherwise). The leaf node **CheckBool** returns **SUCCESS** if the variable **fd_found** is **TRUE**. This would mean that a fire has been detected by the module, and its estimated coordinates are stored at (**fd_x**, **fd_y**, **fd_z**). Otherwise the (sub-)mission fails. If successful, the UAV is commanded to a point 3 meters over the estimated position (computed using the **MathOperationFloat** leaf), by calling to the corresponding **UPOGotoGoal** (Section 4). Once there, the extinguishing procedure with the blanket is activated (**UPOFireExtinguish**, Section 5.3.3).

- **Decorator:** it processes or modifies the status it receives from its child.
- **Leaf:** this is where the actual task is performed, the atomic tasks that the robot can carry out, or other functionalities. As such, these nodes cannot have any children.

As it can be seen from the classification above, BT decouple logic from actual tasks in a natural way. When developing a tree, one only should care about the leaf nodes. In this case, these leaves correspond to the **actionlib** tasks described just above and another potential operations. The flow can later be defined and re-arranged constantly, creating new behaviors and expanding on what is already done. This *modularity* and *composability* (due to the hierarchical nature of the trees) of BTs with respect to alternatives like FSM is one of the advantages of the formulation (Colledanchise, 2018), and was very relevant for defining the missions in the fleet and adapting to the lessons learned during the rehearsals. Missions could be re-defined very fast, and behaviours could be developed in parallel and easily integrated as sub-trees in more complex missions once well tested and validated.

The behavior of the individual robots of the team in the Challenge are designed using BTs. Fig. 8 presents the mission of the M600 robot (extinguishing one outdoor fire and one facade fire) as a BT, combining

associated atomic tasks of navigation, fire detection and fire extinguishing as described above, and the required additional leaf, composite and decorator nodes.

The executive that carries out and monitors the mission defined as a BT uses a BT engine. We have employed a publicly available BT implementation¹¹. We have developed a ROS interface to it. It ships with a library containing ROS subscribers, publishers, services and `actionlib` leaf nodes (mapping adequately the states of these actions to the corresponding states for the nodes BT) to be able to send and receive messages, and call services/actions to/from other nodes running in the network. And it includes a `BT Mission Execution` ROS node that offers an additional interface (as an `actionlib` as well) to load, start and stop user-defined behavior trees. This node (see Fig. 7) runs onboard each robot, providing them with full operational autonomy to carry out complete missions.

6.3 Cooperation and Coordination

The approach to Challenge 3 takes advantage of the use of a heterogeneous robot team (mixing UGV and different types of UAVs). On the one hand, each robot specializes on one of the tasks for the Challenge. This means that we consider a loose cooperation between the robots. In particular, we devote the ground robot for the ground floor indoor fire, and each UAV to a different facade (with the larger M600 for the outside fires and the facade closest to the outside fires).

The Control Station module (Fig. 7) commands the different robots to execute out their missions, and those are carried out autonomously by each robot. Each robot runs all modules onboard, including a different ROS master node. We use the software described in (Tardioli et al., 2019) to share between robots only vital information through the wireless network, including the position of each robot and the interfaces to control the robots from the station.

Thus, the main aspect to consider is the coordination in time and space to avoid collisions. The task allocation mitigates the risks, as the different vehicles will operate in different facades and, thus, different spaces. In any case, it is important to avoid close encounters between the vehicles. The takeoff zone is very narrow, so the Control Station regulate the order of initiating the missions for each vehicle so that no two UAVs take off at the same time. Furthermore, each vehicle has a landing zone that is separated from the rest of the team.

7 Experiments and Results

This section presents the results obtained during the 2020 competition the MBZIRC at the National Exhibition Center in Abu Dhabi, (UAE) (see Figure 1). We describe in detail the results obtained for the different subsystems, as well as the results obtained by the integrated system in the final event.

7.1 Localization results

A map of the arena was built during the first rehearsal day. A DJI M210 with all sensors on-board was flown manually in order to gather the required sensor data for the map, as detailed in Section 3.1. The map presented in Fig. 4 was used into the MCL approach presented in this paper to provide a consistent robot localization for each robot platform.

Figure 9 shows the estimated localization of the DJI M600 during Trials 1 and 2. The localization system was able to provide the correct robot pose in both experiments, and the missions were carried out completely autonomously. The figure also shows the estimated GPS position of the DJI M600 during the experiments

¹¹<https://www.behaviortree.dev>

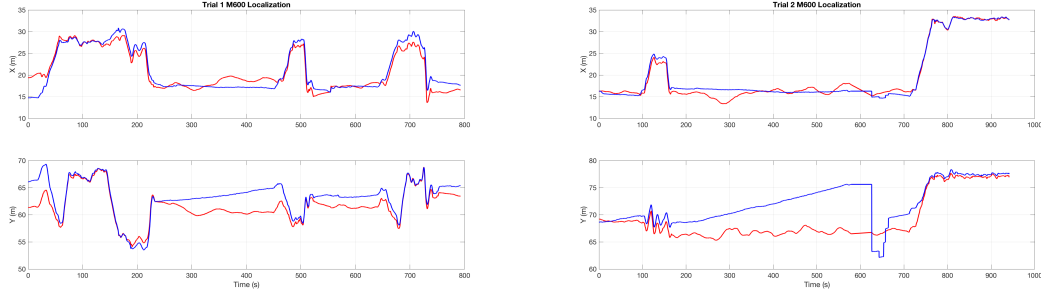


Figure 9: DJI M600 X-Y localization during execution of Trials 1 and 2. (Left) Estimated XY position in Trial 1. (Right) Estimated XY position in Trial 2. Red line denotes the MCL estimation and blue line denotes the GPS estimation.

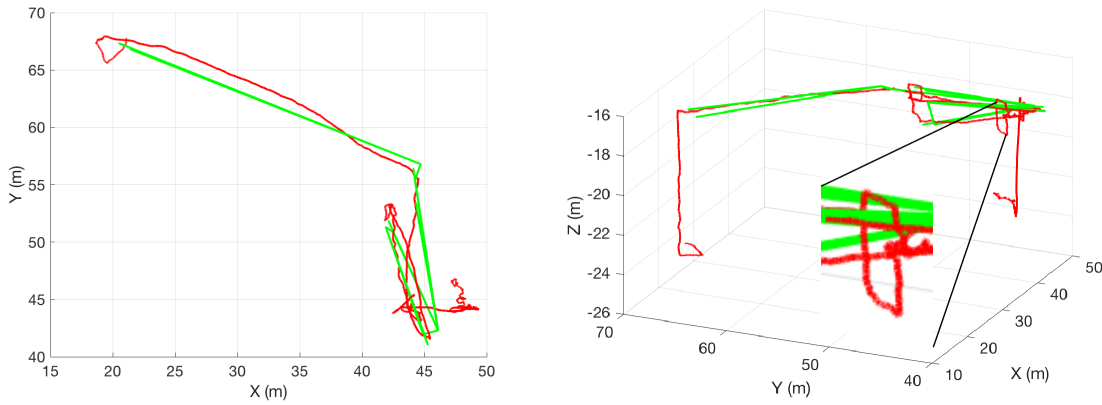


Figure 10: Top view (left) and 3D view (right) of the global planned trajectory (green line) and its associated executed trajectory, as estimated by our localization system (red line) during a flight of the DJI Matrice M210 in the second trial for Challenge 3. Note that the manoeuvre followed during the detection and extinguishing has been zoomed in.

(blue line in the graph). We can see GPS estimation issues in both estimations. Thus, in Fig. 9-right it can be seen how from second 175 to 625 approximately, the GPS estimation evolves at constant velocity in Y axis, with a 15 meters jump in Y at second 625. During this period the drone was landed so the robot position must stay approximately constant. However, the Z estimation of the GPS in the DJI M600 automatically integrates the barometer, so the solution matches very well with the MCL solution (not shown in the figure).

On the other hand, we can see how the GPS estimation also evolves at constant velocity in Y axis from second 225 to 475 approximately in Fig. 9. As previously, the GPS eventually recovers the right estimation, converging to the MCL estimation, which stay stable during the experiment.

The GPS errors presented in Fig. 9 were common during the MBZIRC 2020 execution. This behaviour was detected during the rehearsal days, and we finally decided to significantly reduce the value of w^{gps} from (8).

7.2 Autonomous navigation results

As an example of the performance of our navigation system we present the trajectory of our M210 platform in Trial 2. Figure 10 represents the trajectory followed by the UAV in red alongside with the global planned

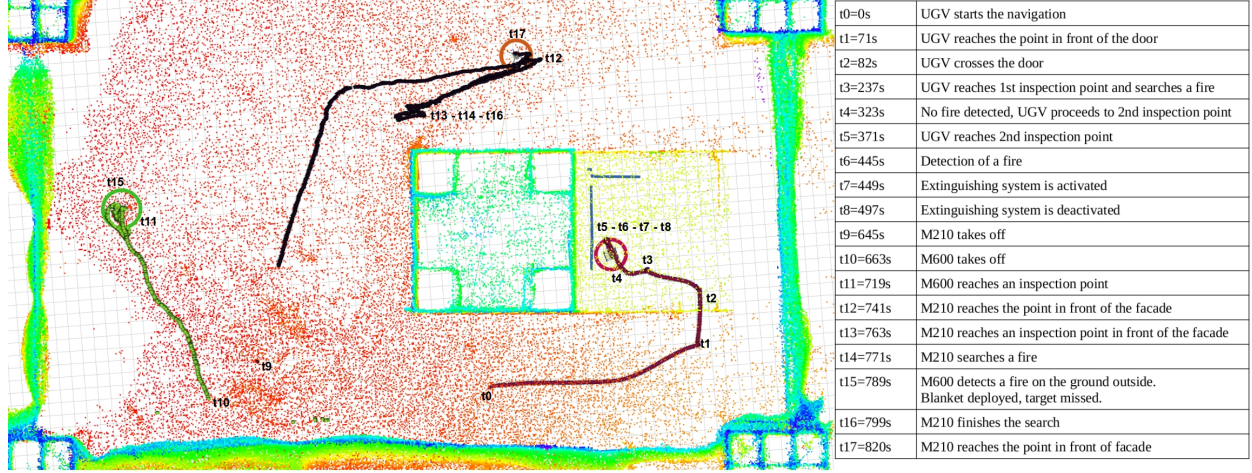


Figure 11: Left: Trajectories of the 3 robots employed in Trial 2. The M600 UAV was tasked with extinguishing an outdoor fire (green trajectory). The M210 UAV was commanded to look and extinguish a fire in the opposite facade of the building (black trajectory). The UGV SIAR was commanded to look and extinguish the indoor fire in the ground floor (red trajectory). Right: Task performed for each robot with the corresponding timestamp.

trajectory in green. As we use a local planner in order to check for unmodeled obstacles on the environment, the tracking of the trajectory on the horizontal plane is not perfect and it tends to take shortcuts on the corners whenever possible. On the other hand, the system follows the altitude reference more closely.

Our planner obtained a remarkable performance that has allowed us to perform the whole challenge without any collisions. The computation times of the global plan is of less than a second in its onboard NUC7i7 and using a single core. On the other hand, the local planner computes trajectories with a workspace of 6x6x2 meters at 7 Hz approximately.

7.3 Results in the MBZIRC competition

The whole integrated multi-robot system was applied 3 times to Challenge 3 during the final event in Abu Dhabi. Twice for the Challenge 3 competition proper (the highest score of both trials in kept as the final score), and once more for the Grand Challenge triathlon (please refer to Section 1.2 for details). The results obtained in the competition are presented in Table 2. With these results, we achieved the seventh place in Challenge 3 (out of 20 teams in the competition) and a third place in the Grand Challenge (out of 17), which combined a reduced version of the three Challenges, in our first participation in the competition. The results highlight the complexity of the challenge. A video highlighting results from the MBZIRC competition can be accessed at <http://robotics.upo.es/mbzirc/skyeye-mbzirc-challenge3.mp4>.

We would like to point out that we scored in all trials in autonomous mode at all times, and that we managed to hit on targets on facade fires and both indoor and outdoor fires. We also managed to autonomously operate a team of 3 robots at the same time. Figure 11 shows the general evolution of Trial 2. In this trial, the ground robot was tasked to look for and extinguish the fire in the ground floor, while the M600 and M210 were tasked to extinguish one outdoor floor with the blanket and one facade fire with water, respectively.

Fig. 12 shows the UGV extinguishing an indoor fire during this Trial 2. As depicted in Fig. 11, the UGV reached several waypoints and one inspection point before reaching the inspection point with the active fire. When the inspection point was reached, the onboard infrared thermal camera checks if a fire exists using the methods of Section 5.1, this is known as the searching phase. If the fire is detected, first a centering action is

Table 2: Results obtained during the MBZIRC 2020 competition. All tasks achieved in autonomous mode. Maximum score for a task is by putting 1 litre or covering 100% of fire.

	Outdoor Fires with blanket (Weights: 10 UAV, 5 UGV)	Facade Fires with UAVs (Weights: 14 ground floor, 8 first and second floor)	Indoor Fires (Weights: 24 second floor, 16 first floor, 10 ground floor))
TRIAL 1	1 fire, with UAV. Weight: 10. 50% covered	None	None
TRIAL 2	None	None	Ground floor, with UGV. Weight: 10. 350 ml.
GRAND	N/A	Ground floor fire, under wind, with UAV. Weight: 14. 8 ml.	Ground floor, with UGV. Weight: 10. 3 ml.

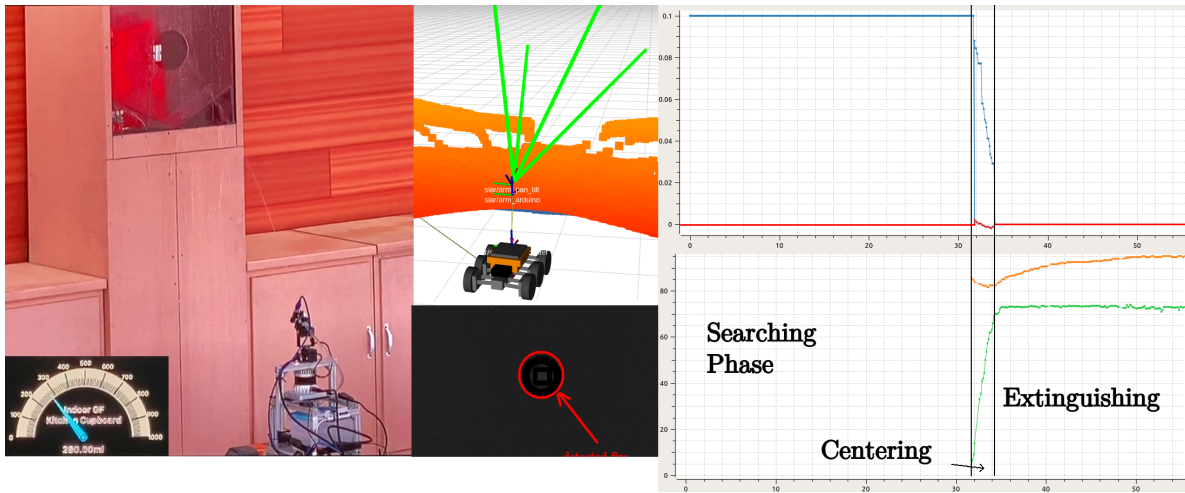


Figure 12: Fire extinguishing action performed by the UGV in Trial 2. (Left) Snapshot of the video recorded by the organization in the extinguishing action. The amount of water poured in can be seen below. (Center, up) Internal state of the SIAR and FOV of the thermal camera. (Center, down) Detected fire on the IR image. (Right) The upper plot represents the pan and tilt velocity commands on blue and red lines, respectively. In the plot at the bottom, the image coordinates are plotted in light green and orange, respectively.

performed and finally a fire extinguishing system is activated after the centering action to deploy 1 litre (see Fig. 12-left), of which 350 ml went on target in Trial 2. Fig. The mission is designed for the ground platform to continue exploring the environment for more fires, to compensate for potential false alarms. This turned out to be too conservative, as the system was actually capable of detecting the real fire present and no false alarms were created. Finally, the robot returns to its initial position when the time is over. The UGV robot was able to deploy water in the correct fire in the ground floor during the Trial 2 and the Grand Challenge.

Fig. 13 depicts the fire blanket mission for the M600 UAV during Trial 2, as described in Fig. 8. In this case, the blanket was deployed but missed the target by a few centimeters. However, during Trial 1 the blanket was successfully deployed over the fire, covering 50% of it. We actually increased the height at which the deployment manoeuvre was performed from Trial 1 to 2 to add some safety buffer, and this was detrimental.

The M210 was able to explore part of the facade looking for the fires, but we ran out of time during Trial 2, as the UAV took off later in during the mission, and it could not extinguish a fire there as the time expired before it could detect any fire. On contrast, in the Grand Challenge day, our M600 drone did manage to partially extinguish a facade fire during the Grand Challenge. It explored several assigned inspection points until it detected an active fire with its thermal camera on front (see Fig. 14, left). As soon as it detected

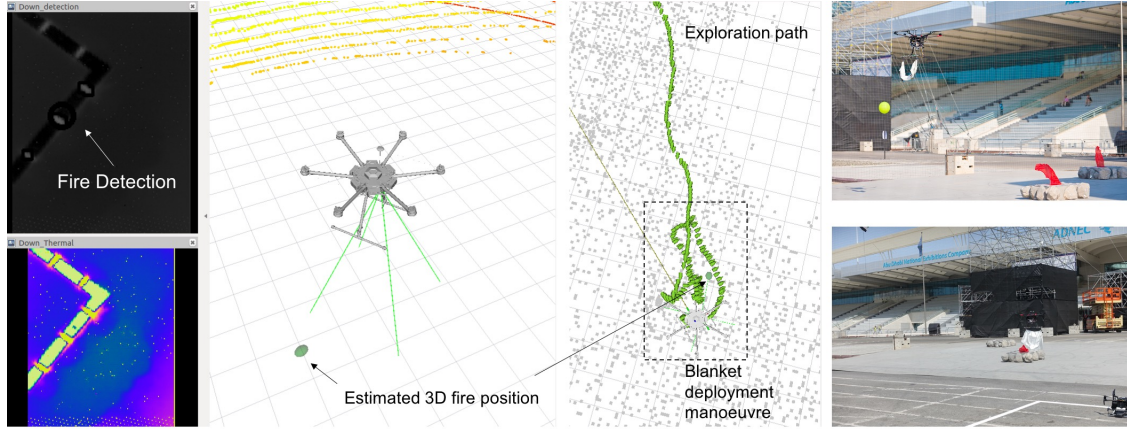


Figure 13: Data from one blanket deployment task. An exploration path is given and the methods of Section 5.1 are used to detect and estimate the 3D position of the fire. Then, the blanket deployment manoeuvre is carried out. Right: two pictures of the exploration (top) and deployment (bottom) phases.

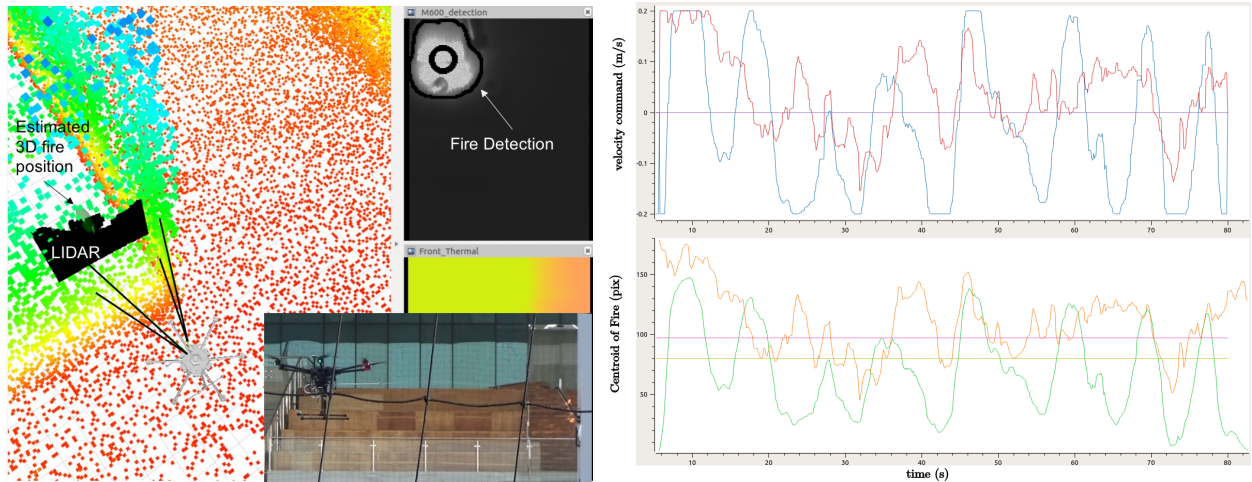


Figure 14: Facade fire extinction. Left: the thermal images are used to detect the fire. The 3D position is estimated by combining the information with LIDAR. Right: visual servoing. Right, top: commanded speeds generated by the control system for water extinguishing on y (horizontal UAV body axis, parallel to the wall, blue) and z (vertical UAV body axis, red). Right, bottom: u (column, green) and v (row, orange) image coordinates of the centroid of the fire detected on the image. The u and v centering coordinates are plotted in pink and light green, respectively.

the fire, it switched into fire centering mode and started to eject water to extinguish the fire.

Fig. 14 right represents the output of our control system as a function of the coordinates of the centroid of the detected fire region on the thermal image. This control system sends velocity commands to the M600 autopilot in order to center the fire in the image. This particular fire was given larger weights as it was subjected to lateral wind gust of up to 8 m/s. It can be seen in Fig. 14 how this provoked oscillations in the control in the lateral velocity, making it difficult to adequately point the water hose. The fire was never completely lost during the water ejection and the fire was considered partially extinguished.

8 Conclusions and Lessons Learnt

We present in this article our entry to tackle MBZIRC Challenge 3: “Team of Robots to FightFire in High Rise Building”, using cooperative multi-robot team framework approach. The system presented achieved the 7th place (same score as 6th, longer mission time) in Challenge 3 and contributed to the 3rd place in the Grand Challenge. The difficulty of this Challenge can be seen in that only 9 teams were able to score in autonomous mode between the two trials of Challenge 3, and only 5 teams during the Grand Challenge trial. We managed to score in autonomous mode in all three occasions. At the same time, the system was not able to perform as robustly as expected and evidently some other teams did better. Some of the lessons learned are presented here:

Being a robotics competition means that not only software matters, but hardware selection and design decisions are key. The use of off-the-shelf platforms was a good decision, in particular for the drones. The DJI platforms offered a ready to fly system with direct ROS integration. This opened the door to focus on the software development tools required for the robot autonomy, significantly reducing the issues and problems derived from hardware integration in drones. It is also worth to mention that the we experimented DJI software issues before and during the competition: onboard firmware mismatch problems, random GPS no-fly area restrictions and motor overheating. Nevertheless, all in all, we consider that the advantages of using a commercial off-the-shelf drone platform was a good decision and that, in general, is preferable to avoid the design/implementation of drones in order to focus in the autonomy problem. The platforms were adapted for the water ejection and blanket deployment. The water ejection mechanisms were adequate, even though achieving a higher pressure would have helped. Regarding the blanket deployment mechanism, while we were able to deploy the blanket on the fire once, we were not able to achieve a fully satisfactory system less affected by the air turbulence generated by the own UAV. Finally, our ground robot used a pan and tilt unit instead of an arm like most teams for budgetary and weight restrictions. The use of an arm clearly helps in the final extinguishing manoeuvre.

Using a map-based localization system allowed us a lot of versatility, even permitting us finally discarding the use of GPS for localization. This approach allowed us for fast system deployment, so that we do not need a precise GPS localization to localize the robot into the map, just the minimum required by the DJI drones to perform the take-off maneuver safely. The localization had a stable performance and a good precision during the competition, relying only on the use of LIDAR measures that were matched against a 3D map obtained a priori. It also was very important in order to be able to safely navigate in the scenario, as the localization of our platforms was performed taking into account the different elements on the stage, e.g. columns or safety nets, allowing us to locate them with good precision against the obstacles in the environment. The localization supported the robot autonomous navigation in the scenario, and the map-based system made the indoor-outdoor transition on localization seamless. However, only the ground robot entered the building. Even though we performed missions with the drones inside the building in simulation, finally we did not attempt to enter the building during the competition. Actually, no team was able to score inside the building during the competition, and only some manual trials were performed. This clearly requires techniques with a higher level of maturity.

Robot local autonomy was also key. Each robot was able to carry out its mission with all processing carried out on board, with the central station only in charge of launching the local missions of the robots in adequate order and relaying some global information. Even under communication dropouts, the robots were able to carry out their missions. The use of BTs as a mission executive on board the robots offered us also a great deal of flexibility to design and compose the missions on the base of the atomic tasks and sub-behaviours already defined. The BT engine also allowed the robots to react to the events detected during the runs.

At the same time, robustness is fundamental to operate three to four robots at the same time. During trials, preparation time was very short, and all systems needed to be able to boot by clicking a switch. While we were able to perform missions with 3 robots at the same time, the robustness achieved during mission start-up was not enough to fully leverage the 15 minutes of the missions, and some times, delays prevented

to achieve more tasks in the mission. However, we feel that we are in the right direction and we look forward to subsequent editions to improve the robustness and accuracy of our systems and to, hopefully, win the challenge!

Acknowledgments

This work has been supported by the Spanish Ministry of Science, Innovation and Universities (COMCISE RTI2018-100847-B-C22, MCIU/AEI/FEDER, UE) and the Khalifa University under contract no. 2020-MBZIRC-10. The work of S. Martinez-Rozas is partially supported by the Antofagasta University.

UPO would like to acknowledge Paulo Alvito and the IDMind¹² company for the support with the ground robot hardware, Marcel Richter and the AeroGuillena airfield for the support during the tests, and Danilo Tardioli, from the University of Zaragoza, Spain, for his multi-master ROS software for multi-robot teams.

References

- Agarwal, S., Mierle, K., and Others (2012). Ceres solver. <http://ceres-solver.org>.
- Alejo, D., Mier, G., Marques, C., Caballero, F., Merino, L., and Alvito, P. (2020). Siar: A ground robot solution for semi-autonomous inspection of visitable sewers. In *Advances in Robotics Research: From Lab to Market*, pages 275–296. Springer.
- Amano, H., Osuka, K., and Tarn, T. . (2001). Development of vertically moving robot with gripping handrails for fire fighting. In *Proceedings of the IEEE/RSJ International Conference on Intelligent Robots and Systems (IROS)*, volume 2, pages 661–667.
- Ambrosia, V. G., Wegener, S. S., Sullivan, D. V., Buechel, S. W., Dunagan, S. E., Brass, J. A., Stoneburner, J., and Schoenung, S. M. (2003). Demonstrating uav-acquired real-time thermal data over fires. *Photogrammetric engineering & remote sensing*, 69(4):391–402.
- Ando, H., Ambe, Y., Ishii, A., Konyo, M., Tadakuma, K., Maruyama, S., and Tadokoro, S. (2018). Aerial hose type robot by water-jet for fire fighting. *IEEE Robotics and Automation Letters*, 3:1128–1135.
- Bailon-Ruiz, R., Lacroix, S., and Bit-Monnot, A. (2018). Planning to monitor wildfires with a fleet of uavs. In *2018 IEEE/RSJ International Conference on Intelligent Robots and Systems (IROS)*, pages 4729–4734. IEEE.
- Bradshaw, A. (1991). The UK security and fire fighting advanced robot project. In *IEE Colloquium on Advanced Robotic Initiatives in the UK*.
- Casbeer, D. W., Kingston, D. B., Beard, R. W., and McLain, T. W. (2006). Cooperative forest fire surveillance using a team of small unmanned air vehicles. *International Journal of Systems Science*, 37(6):351–360.
- Colledanchise, M. (2018). Behavior trees in robotics and al. *ArXiv*.
- Colledanchise, M. and Ogren, P. (2017). How behavior trees modularize hybrid control systems and generalize sequential behavior compositions, the subsumption architecture, and decision trees. *IEEE Transactions on Robotics*, 33(2):372–389.
- Delmerico, J., Mintchev, S., Giusti, A., Gromov, B., Melo, K., Horvat, T., Cadena, C., Hutter, M., Ijspeert, A., Floreano, D., Gambardella, L. M., Siegwart, R., and Scaramuzza, D. (2019). The current state and future outlook of rescue robotics. *Journal of Field Robotics*, 36:1171–1191.

¹²<https://www.idmind.pt>

- Dias, A., Capitan, J., Merino, L., Almeida, J., Lima, P., and Silva, E. (2015). Decentralized target tracking based on multi-robot cooperative triangulation. In *IEEE International Conference on Robotics and Automation, ICRA*, page 3449–3455.
- Hornung, A., Wurm, K. M., and Bennewitz, M. (2010). Humanoid robot localization in complex indoor environments. In *IEEE/RSJ International Conference on Intelligent Robots and Systems (IROS)*.
- Maza, I., Caballero, F., Capitan, J., Martinez-de Dios, J. R., and Ollero, A. (2011). Experimental results in multi-UAV coordination for disaster management and civil security applications. *Journal of Intelligent & Robotic systems*, 61(1-4):563–585.
- MBZIRC (2020). Mohamed Bin Zayed International Robotics Challenge - The Challenge 2020. <https://www.mbzirc.com/challenge/2020>.
- Merino, L., Caballero, F., Martínez-de Dios, J. R., Ferruz, J., and Ollero, A. (2006). A cooperative perception system for multiple uavs: Application to automatic detection of forest fires. *Journal of Field Robotics*, 23(3-4):165–184.
- Merino, L., Caballero, F., Martínez-De-Dios, J. R., Maza, I., and Ollero, A. (2012). An unmanned aircraft system for automatic forest fire monitoring and measurement. *Journal of Intelligent & Robotic Systems*, 65(1-4):533–548.
- Michael, N., Shen, S., Mohta, K., Kumar, V., Nagatani, K., Okada, Y., Kiribayashi, S., Otake, K., Yoshida, K., Ohno, K., et al. (2014). Collaborative mapping of an earthquake damaged building via ground and aerial robots. In *Field and service robotics*, pages 33–47. Springer.
- Mohta, K., Watterson, M., Mulgaonkar, Y., Liu, S., Qu, C., Makineni, A., and Kumar, V. (2018). Fast, autonomous flight in gps-denied and cluttered environments. *Journal of Field Robotics*, 35:101–120.
- Molina, M., Carrera, A., Camporredondo, A., Bavle, H., Rodriguez-Ramos, A., and Campoy, P. (2020). Building the executive system of autonomous aerial robots using the aerostack open-source framework. *International Journal of Advanced Robotic Systems*, 17(3):1729881420925000.
- Nash, S. K. and Tovey, C. (2010). Lazy theta*: Any-angle path planning and path length analysis in 3d. In *Proceedings of the Twenty-Fourth AAAI Conference on Artificial Intelligence (AAAI)*, page 147–154.
- Ogren, P. (2012). Increasing modularity of uav control systems using computer game behavior trees. In *Aiaa guidance, navigation, and control conference*, page 4458.
- Paxton, C., Hundt, A., Jonathan, F., Guerin, K., and Hager, G. D. (2017). Costar: Instructing collaborative robots with behavior trees and vision. In *IEEE International Conference on Robotics and Automation (ICRA)*, page 564–571.
- Perez-Grau, F., Caballero, F., Merino, L., and Viguria, A. (2017). Multi-modal mapping and localization of unmanned aerial robots based on ultra-wideband and rgb-d sensing. In *IEEE/RSJ International Conference on Intelligent Robots and Systems (IROS)*.
- Perez-Grau, F., Ragel, R., Caballero, F., Viguria, A., and Ollero, A. (2018). An architecture for robust uav navigation in gps-denied areas. *Journal of Field Robotics*, 35(1):121–145.
- Pratt, J. and Manzo, J. (2013). The DARPA robotics challenge. *IEEE Robotics & Automation Magazine*, 20:10–12.
- Quigley, M., Gerkey, B., Conley, K., Faust, J., Foote, T., Leibs, J., Berger, E., Wheeler, R., and Ng, A. (2009). Ros: an open-source robot operating system. In *Proc. of the IEEE Intl. Conf. on Robotics and Automation (ICRA) Workshop on Open Source Robotics*, Kobe, Japan. <http://ros.org>.
- Rusinkiewicz, S. and Levoy, M. (2001). Efficient variants of the icp algorithm. In *Third International Conference on 3D Digital Imaging and Modeling (3DIM)*, Quebec City, Canada.

- Schneider, F. E. and Wildermuth, D. (2017). Using robots for firefighters and first responders: Scenario specification and exemplary system description. In *2017 18th International Carpathian Control Conference (ICCC)*, pages 216–221. IEEE.
- Sheh, R., Schwertfeger, S., and Visser, A. (2016). 16 years of robocup rescue. *KI-Künstliche Intelligenz*, 30:267–277.
- Shen, S., Mulgaonkar, Y., Michael, N., and Kumar, V. (2014). Multi-sensor fusion for robust autonomous flight in indoor and outdoor environments with a rotorcraft mav. In *2014 IEEE International Conference on Robotics and Automation (ICRA)*, pages 4974–4981. IEEE.
- Skeele, R. C. and Hollinger, G. A. (2016). Aerial vehicle path planning for monitoring wildfire frontiers. In *Field and Service Robotics*, pages 455–467. Springer.
- Tardioli, D., Parasuraman, R., and Ögren, P. (2019). Pound: A multi-master ros node for reducing delay and jitter in wireless multi-robot networks. *Robotics and Autonomous Systems*, 111:73–87.
- Thrun, S., Fox, D., Burgard, W., and Dellaert, F. (2001). Robust monte carlo localization for mobile robots. *Artificial Intelligence*, 128(1):99 – 141.
- TrinityCollege (2020). Trinity College International Fire Fighting Robot Contest. <https://trinityrobotcontest.org/>.
- Usenko, V., von Stumberg, L., Stücker, J., and Cremers, D. (2020). Tum flyers: Vision—based mav navigation for systematic inspection of structures. In *Bringing Innovative Robotic Technologies from Research Labs to Industrial End-users*, pages 189–209. Springer.
- Winfield, A. F., Franco, M. P., Brueggemann, B., Castro, A., Ferri, G., Ferreira, F., Liu, X., Petillot, Y., Roning, J., Schneider, F., et al. (2017). euRathlon and ERL emergency: A multi-domain multi-robot grand challenge for search and rescue robots. In *Iberian Robotics conference*, pages 263–271. Springer.
- Yamada, Y. and Nakamura, T. (2016). Ummanned fire-fighting aerial vehicle to enable continuous water discharge. In *JSME Conference on Robotics and Mechatronics*.
- Zhang and Singh, S. (2014). LOAM: Lidar Odometry and Mapping in Real-time. In *Robotics: Science and Systems Conference (RSS)*.
- Zhang, J. and Singh, S. (2017). Low-drift and real-time lidar odometry and mapping. *Auton. Robots*, pages 401–416.